VOLUME 15 ISSUE 2

LIDAR MAGAZINE

SPRING 2025

SPECIAL ISSUE

UNDERWATER MAPPING

10 EVOLUTION OF MULTIBEAM SONAR
A review of the complex array of components required for high-quality hydrographic data collection and management

20 AIRBORNE LIDAR TUTORIAL: PART III
The third of a four-part tutorial addresses bathymetric lidar, reviewing core challenges and the systems currently on market

48 BOOK REVIEW: 25¢ PIANO LESSONS
Examining the autobiography of Dr. David Maune, lidar luminary; an eight-decade chronicle of geospatial development and triumph

AIRBORNE LIDAR

A Tutorial for 2025

Part III: Bathymetric lidar

Airborne laser bathymetry (ALB), also referred to as bathymetric laser scanning or bathymetric lidar, is a technique to measure the depths of shallow coastal or inland water using a pulsed, scanning laser. While the infrared wavelengths used for topographic lidar cannot penetrate water, wavelengths in the green and blue spectrum of visible light are suitable, as signal attenuation is least for wavelengths around 460-550 nm. Most bathymetric lidar sensors use a wavelength of λ=532 nm, which is the result of frequency-doubling a conventional Nd:YAG infrared laser operating at λ=1064 nm. Since the invention of lasers in the 1960s, there have also been reports on the use of green lasers. While underwater object detection was the first application, ALB is mostly used today for surveying and monitoring shallow coastal areas, harbor facilities, and shipping channels. The increased measurement rates of today's sensors also allow the use of this active remote sensing method for the mapping and monitoring of smaller standing or running inland waters.

Measuring principle

A laser mounted on an airborne platform (fixed-wing aircraft, helicopter, unmanned aerial vehicle) emits very short laser pulses in the green wavelength range. The laser pulse passes through the atmosphere, possibly interacts with objects above the body of water (vegetation, power lines, etc.) and then hits the water surface. There, the laser beam is reflected on the one hand and refracted on the other when it enters the optically denser medium of water at the air-water interface. The direction of the deflected beam depends on the incidence angle at the water surface and on the refractive indices in air and water. The relation between incoming (air-sided) and outgoing (water-sided) ray direction and speed of light is described by Snell's law of refraction:

$$\frac{\sin \alpha_L}{\sin \alpha_W} = \frac{n_W}{n_L} = \frac{c_L}{c_W} \quad \text{EQ1}$$

α_L and α_W denote the angles between the water surface normal direction and the air-sided (α_L) and water-sided (α_W) laser beam, c_L and c_W are the laser pulse propagation velocities in air and water, and n_L and n_W are the corresponding refractive indices. The refractive index in a vacuum is 1.0, in dry air (15 °C, 1013.25 mbar) around 1.0003, and in clear water 1.333. Please note that the refractive index in water is slightly different for angular deflection and the propagation velocity. For the former, the phase velocity of the inherent laser light is crucial, and for the latter, the group velocity of the laser pulse.

Within the water column, the laser light interacts with the water and suspended sediment particles, and the signal is both scattered and absorbed. Continuous forward scattering leads to a hyperbolic conical expansion of the laser spot size with increasing water depth. Volume backscattering, in turn, causes reflection of the laser signal from the water column back to the receiver, where the recorded amplitude drops asymmetrically after the first peak from the water surface. Part of the laser radiation finally reaches the bottom of the water body (seabed, river bottom, etc.), where it is reflected and partially

BY GOTTRIED MANDLBURGER

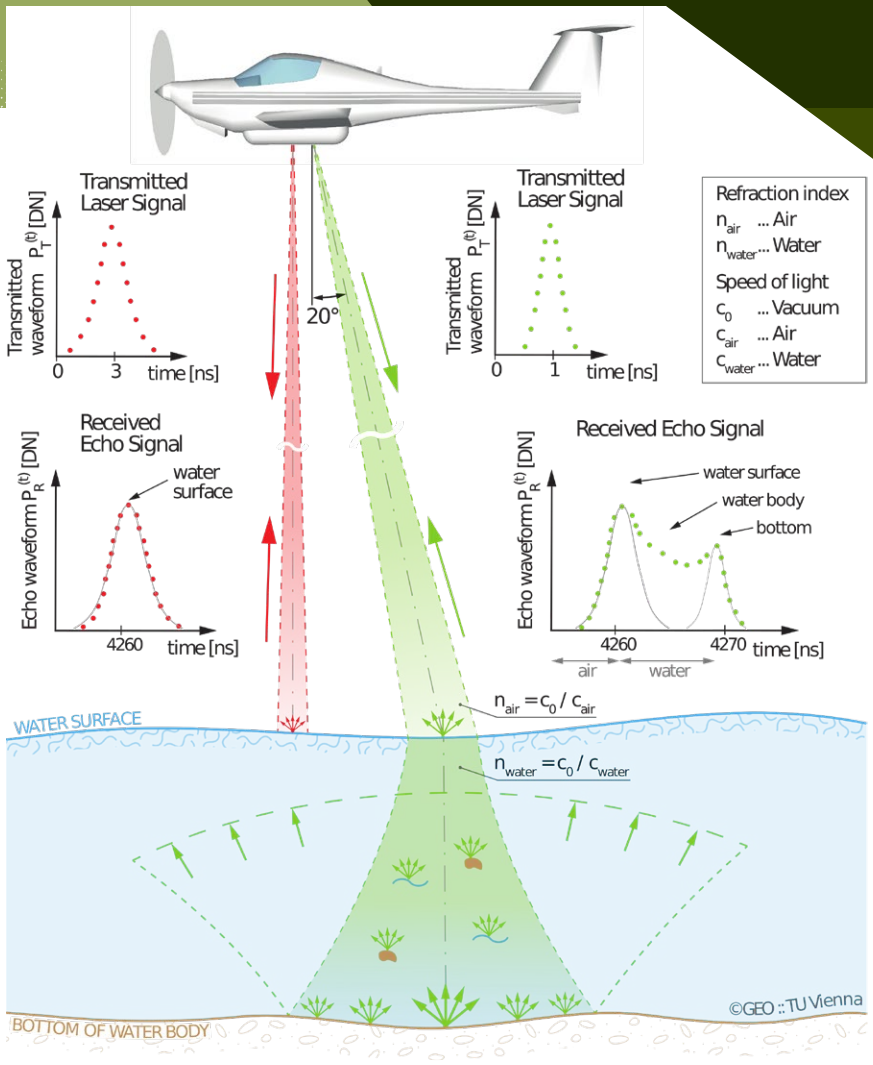

Figure 1: Setup and specifications of selected integrated lidar-camera sensors; laser footprint and image GSD are reported for a flying altitude of 1000 m.

absorbed, depending on the reflectance of the bottom material. After the return trip through the water column and atmosphere, a small proportion of the emitted radiation reflected from the bottom reaches the receiver. In a similar way to topographic laser scanning, the roundtrip time can be measured by registering the time stamps of the emitted pulse and the received echo (discrete echo systems). Due to the complex interaction of the radiation at the air-water interface, in the water columns, and at the bottom, however, most of the available ALB sensors record the entire waveform (outgoing pulse and received echo response) discretized in time with a sampling rate of 1-5 GHz. The waveforms can be evaluated either online during the flight or in post-processing, if the digitized signal is also stored on disk. In both cases, waveform analysis provides radiometric information in addition to the roundtrip time (distance). Next to the measurement range, the signal intensity depends on atmospheric parameters (humidity), roughness of the water surface, water turbidity, water depth, and reflectivity of the bottom surface. The relationships are schematically sketched in **Figure 1**.

Interaction of laser light with water

In Part I of this tutorial, we discussed the general relation between the transmitted power P_T and the received power P_R. For extended targets, i.e. targets larger than the laser footprint, we can simplify the laser-radar equation as:

$$P_R = \frac{P_{Tf}}{4\pi R^2}\,\sigma + P_{BK} \qquad \text{EQ2}$$

In Equation 2, P_{Tf} summarizes all parameters, which can be considered constant for a single flight mission, namely the transmitted power P_T, the diameter of receiver's aperture D, and the atmospheric and sensor-specific loss factors η_{ATM} and η_{SYS}.

$$P_{Tf} = P_T\, D^2\, \eta_{ATM}\, \eta_{SYS} \qquad \text{EQ3}$$

The remaining parameters influencing the received power P_R are the measurement range R and the backscattering

cross-section σ. The latter incorporates all target properties, i.e. reflectance and backscattering solid angle (cf. Part I, Equation 3).

Attenuation of the laser radiation occurs within the atmosphere, but for the most part in the medium of water. As stated above, when the green laser signal hits the water surface, part of the signal is reflected at the air-water interface, while the remaining part penetrates the water body and reflects off the bottom. For laser beams hitting water, we can further separate the signal contributions from the water surface (P_{WS}), the water column (P_{WC}), the bottom of the water body (P_{WB}), and background radiation P_{BK}.

$$P_R = P_{WS} + P_{WC} + P_{WB} + P_{BK} \quad \text{EQ4}$$

The following Equations 5-7 describe the individual contributions from (i) the water surface, (ii) the water column, and (iii) the water bottom, summarized in Equation 4:

$$P_{WS} = \frac{P_{Tf} L_O}{4R^2} \quad \text{EQ5}$$

$$P_{WC}(r_w) = \frac{P_{Tf} F (1 - L_O)^2 \beta(\varphi) e^{-2kr_w}}{4(n_W R + r_w)^2} \quad \text{EQ6}$$

$$P_{WB}(r_w) = \frac{P_{Tf} F (1 - L_O)^2 R_B e^{-2kr_w}}{4(n_W R + r_w)^2} \quad \text{EQ7}$$

The fraction of the total received signal strength reflected from the water surface P_{WS} is described by surface albedo L_O, which in turn depends on the roughness of the water surface and the incidence angle between the laser beam and the water surface normal direction. As laser beams hitting the water surface orthogonally produce a very strong backscatter, which may lead to saturation at the receiver, bathymetric laser scanners typically employ conical scanning with a constant off-nadir angle of around 15-20°. Due to the high proportion of specular reflection, direct reflections from the water surface can only be detected when the surface is slightly ruffled. P_{WS} is also dependent on the volume scattering function β(φ).

The signal from the water column P_{WC} depends on the underwater measurement range r_w and is dominated by scattering and absorption described by the diffuse attenuation coefficient k that characterizes the optical properties of water (i.e. turbidity). n_w is the refractive index of water and is a loss factor to account for the fact that not all of the backscattered energy reaches the detector (see **Figure 1**). In addition to all the parameters described above, the contribution from the water bottom P_{WB} is influenced by the seabed reflectance R_B. Light-colored sand (coastal areas) or gravel (inland rivers) have a high reflectivity and thus favor depth penetration. In contrast, muddy soil or dark, submerged vegetation have a negative effect on the achievable depth.

Refraction correction

As explained above, laser bathymetry is a two-media measurement method. The laser beam is deflected at the air-water interface and the propagation speed decreases on entering the optically denser medium of water. For the calculation of precise 3D point coordinates of the water bottom, the intersection point of the laser beam with the water surface must be determined for each laser pulse. In addition, the magnitude and orientation of the tilt of the water surface are also required. The refraction point can be determined individually for each laser pulse, if both the water surface and the water bottom can be identified from the waveform of the backscattered echo signal. This is especially the case for the classic ALB sensor design with coaxial emission of the primary infrared and the green laser radiation derived from it. The infrared channel provides information from the water surface, but does not penetrate the water body. The green channel, in turn, provides information from the water bottom and can also contain reflections from the water surface.

Depending on the actual incidence angle between laser beam and water surface normal direction, however, it may not be possible to detect an echo from the water surface in either the green or infrared channel. This applies especially to very smooth water surfaces (e.g., an inland lake on a calm day) or to situations where the laser beam hits the side of a water wave front facing away from the sensor. For small-footprint bathymetric sensors in particular, the coaxial emission of both wavelengths is no longer the default. Instead, separate infrared scanners with nadir alignment are used, because the backscattered signal strength from the water surface is particularly high when the laser beams hit the water surface orthogonally due to the mirror-like reflection. Some scanners also do without the infrared channel altogether. In most cases, therefore, refraction correction is based on a gridded 2.5D model of the water surface, which is interpolated from all available surface reflections. While a static water surface can be assumed for standing and running inland waters, the dynamics of the water surface must be taken into account for applications in coastal areas in order to consider wave movements. For the latter, the surface

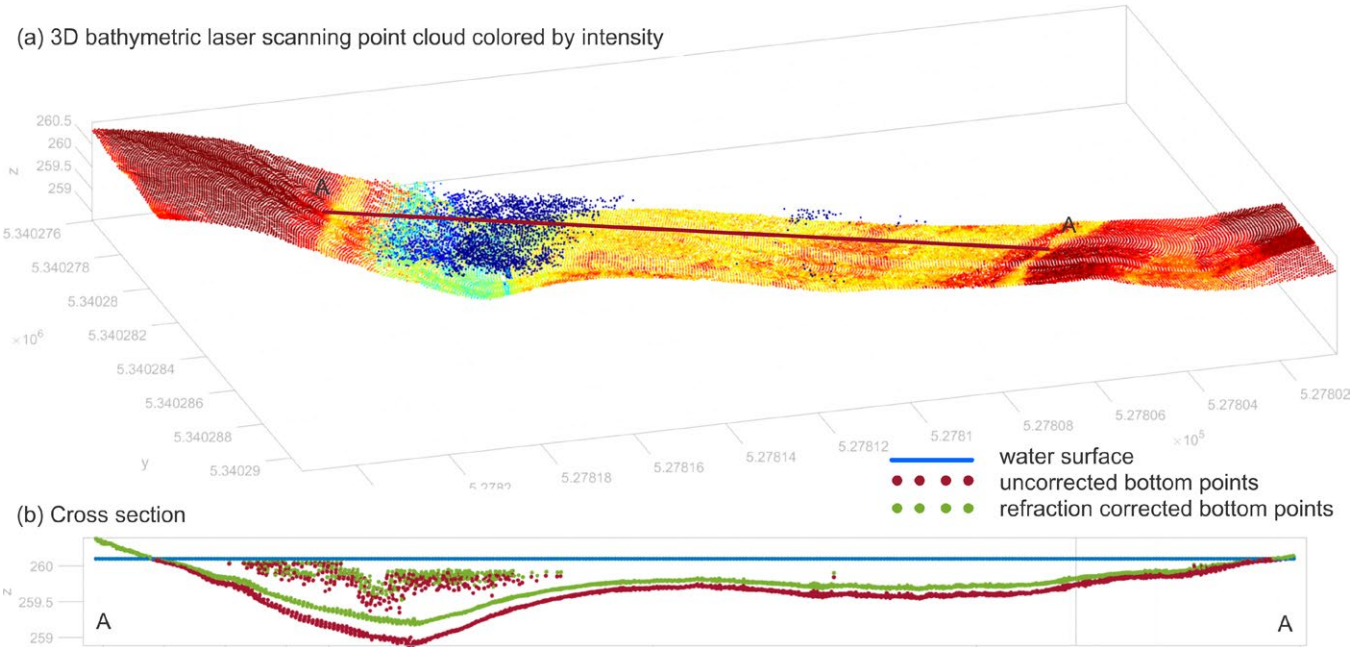

Figure 2: Raw and refraction-corrected bathymetric laser scanning points of a river section. (a) perspective view of raw laser points colored by intensity (red=high, blue = low); (b) cross section showing modeled water surface (blue), raw laser points (red) and refraction-corrected points (green).

model may only be calculated from temporally adjacent laser echoes.

In practice the refraction correction is carried out by applying Snell's law of refraction. For this purpose, the intersection point between the laser beam and the water surface model must first be determined. The laser line is defined by the origin and the beam direction. Ray tracing of the laser line and intersection with the water surface grid model yields the intersection point where the beam is deflected. According to Snell's law of refraction, the water-sided incidence angle (α_W) can be calculated from Equation 1 based on the known air-sided incidence angle α_L and the refractive indices in air and water (n_L, n_W). The distance traveled within the water column results from the time difference between the total travel time and the travel time in the atmosphere. The flight time in the atmosphere is calculated based on the known distance between the origin of the laser and the point of intersection with the water surface, as well as the speed of light in the air. Knowing the reduced propagation speed (group velocity) in water and the direction of the underwater laser ray, refraction-corrected 3D positions of the bottom points can be calculated.

Figure 2 shows the raw and refraction-corrected points for a short river section. As can be seen from the raw laser points plotted in **Figure 2a** in a perspective view colored by intensity, the point cloud contains seamless points of the river bed and the dry bank area. The intensity of the points decreases with increasing water depth. In addition to the ground points, some points from the water surface and the water column are also recorded, all with relatively low intensity (blue). Note that there is no continuous coverage with water surface points. Especially in the very shallow part of the section, water surface points are missing and extrapolation is necessary to obtain a continuous water surface model. **Figure 2b** shows the modeled water surface (blue) along with the raw (red) and the refraction-corrected (green) water bottom laser points. It is clearly visible that (i) the corrected points are less deep in general due to the slower propagation speed in water and (ii) the amount of the correction scales with water depth.

Depth penetration and general sensor concepts

In addition to the water's optical properties, the achievable depth of penetration also depends to a large extent on device-specific parameters. The most important influencing factors are the size of the transmitting and receiving optics and their efficiency, the quality of the electronic and electro-optical

Instrument	ATLAS/ICESat-2	CZMIL Supernova	HawkEye-5	CoastalMapper
Manufacturer	Sigma Space	Teledyne Geospatial	Leica Geosystems	Leica Geosystems
Country	U.S.A.	Canada	Switzerland/ Sweden	Switzerland/ Sweden
Carrier platform	satellite	aircraft	aircraft	aircraft
Weight [kg]	298	>300	~280	~150
Dimensions [cm]	n/s	89 x 60 x 90	2x ~ 50 x 50 x 60	66 x 59 x 64
Laser channels [nm]	6x 532	532/7x 532/1064	515/515/1064	515/1030/1064
Camera	no camera	RGB	RGBI	RGBI
Measurement rate [kHz]	10	30/210/240	40/200/500	1000/2000
Pulse energy [mJ]/ laser class	0.2-1.2	class 4	n/s	class 4
Pulse duration [ns]	1.5	1.65	n/s	n/s
Field of view [°]	nadir	40	40	50
Beam divergence [mrad]	0.035	2/5	7.5/4.75/0.5	2.75
Flying altitude [m]	~470,000	400-800	400-600	600-900
Laser footprint [cm]	1400	75-400	190-600	165-250
Scan pattern	no scanning	circular	elliptical	circular
Depth performance [SD]	1	2/3	2/2.5	2.2
Detection technology	single-photon	full waveform	full waveform	full waveform

Table 1: Key parameters of spaceborne, airborne and UAV-borne topobathymetric laser scanners.

components (e.g., receiving diodes, A/D converters) and the transmitted laser power. Sensor manufacturers specify the performance of a bathymetric laser scanner as factors related to either the Secchi depth or the diffuse attenuation coefficient *k*. The Secchi depth (SD), named after the 19th century Italian priest and astronomer Angelo Secchi, is an empirical measure that characterizes water turbidity and denotes the water depth at which a white or black-and-white disc with a diameter of 20–30 cm is no longer visible to the naked eye.

Typical SDs are 10–25 m for very clear coastal waters, 3–10 m for alpine rivers and lakes with clear water, 0.5–1.5 m for larger rivers with high sediment content or coastal areas with strong currents (e.g., North Sea). Depending on the application, ALB sensors can be roughly divided into two classes. For the measurement of shallow water zones with water depths <10 m, systems with short pulse lengths (1-2 ns), low beam divergence (0.7-2 mrad) and low laser power are used. Short pulse lengths make it possible to distinguish echoes from the water surface and from the ground even in very shallow areas with water depths of ≤20 cm. The relatively low beam divergence (e.g., 1 mrad = diameter of the laser scan spot of 50 cm at an altitude of 500 m) also ensures good horizontal resolution. Typically, such systems have a high measurement frequency (> 100 kHz), but are limited in the maximum achievable penetration depth (1-2 SD) due to the comparatively low laser power. They are referred to as topobathymetric laser scanners because, in addition to measuring water depths, they can also capture the topography of the dry part of the littoral area, enabling a seamless transition between water and land (see **Figure 2**).

In contrast, purely bathymetric sensors aim for a maximum penetration depth. Systems in this class use high-power lasers. The higher energy is achieved mainly by a longer pulse duration (approximately 7 ns). To ensure eye safety, the laser beam is widened. A typical beam divergence of 7 mrad corresponds to a laser scan spot (footprint) diameter of 3.5 m on the water surface

	VQ-880-GII	VQ-860-G	VQ-840-GL	Navigator	ABS-SR
	RIEGL LMS	RIEGL LMS	RIEGL LMS	YellowScan	Fraunhofer IPM
	Austria	Austria	Austria	France	Germany
	aircraft	helicopter	UAV	UAV	UAV
	65	18.5	10.5	3.7	2.5
	45 x 45 x 69	47x 28 x 20	36 x 28 x 20	35 x 16 x 19	32 x 18 x 15
	532/1064	532	532	532	532/1064
	RGBI	RGB	RGB	RGB	---
	700/900	50-100	50-200	20	35
	class 3B	class 3B	class 3B	0.005 / class 3B	class 2M
	1.5	1.5	1.5	0.850	~1
	40	40	40	40	30
	0.7-2.0	1-6	1-6	4	constant
	600-700	150-500	50-300	50-100	15
	42-140	15-300	5-180	20-40	5
	circular	elliptical	elliptical	linear	elliptical
	1.5	2.5	2.0	2.0	1.5
	full waveform	full waveform	full waveform	full waveform	full waveform

from a flying altitude of 500 m. The typical measurement frequencies of around 30-40 kHz are significantly lower than for topobathymetric systems. With such sensors, penetration depths of about 3 SD can be achieved, which corresponds to a depth of about 50 m in very clear water.

For all systems, the achievable penetration depth also depends on the angle of incidence on the water surface. While most of the energy is scattered back from the water surface by specular reflection when the laser beam hits the water orthogonally, an angle of incidence of about 20° has proven to be an optimal compromise for capturing both the water surface and the bottom (see **Figure 1**). For this reason, Palmer scanners producing a circular scan pattern are generally used in laser bathymetry, since each emitted laser beam hits the water surface at an approximately constant angle of incidence.

Sensors and platforms

Sensors for recording bathymetry alone or topography and bathymetry together are now used on a variety of carrier platforms such as satellites, aircraft, helicopters and UAVs. The ATLAS (Advanced Topographic Laser Altimeter System) sensor aboard the ICESat-2 satellite is an example of a spaceborne laser sensor with bathymetric capabilities. ATLAS uses single-photon lidar technology. Its prime application is capturing the Earth's cryosphere, but as the sensor uses a green laser (λ=532 nm), it also delivers shallow water bathymetry with a moderate penetration capability of around 1 SD. ICESat-2 data are often used as reference for spectrally derived bathymetry based on optical satellite images, for example, Sentinel-2. High-resolution underwater mapping is not possible with this system due to the large laser footprint diameter (14 m) and the missing scanning mechanism.

At the other end of the scale spectrum, UAV-borne laser bathymetry sensors have been commercially available since around 2018. Compact topobathymetric scanners enable the highest possible spatial resolution with laser footprint sizes in the decimeter range and potential point densities up to 100 points/m^2 and more. The downside of drone-based acquisition of bathymetry data is the areal coverage,

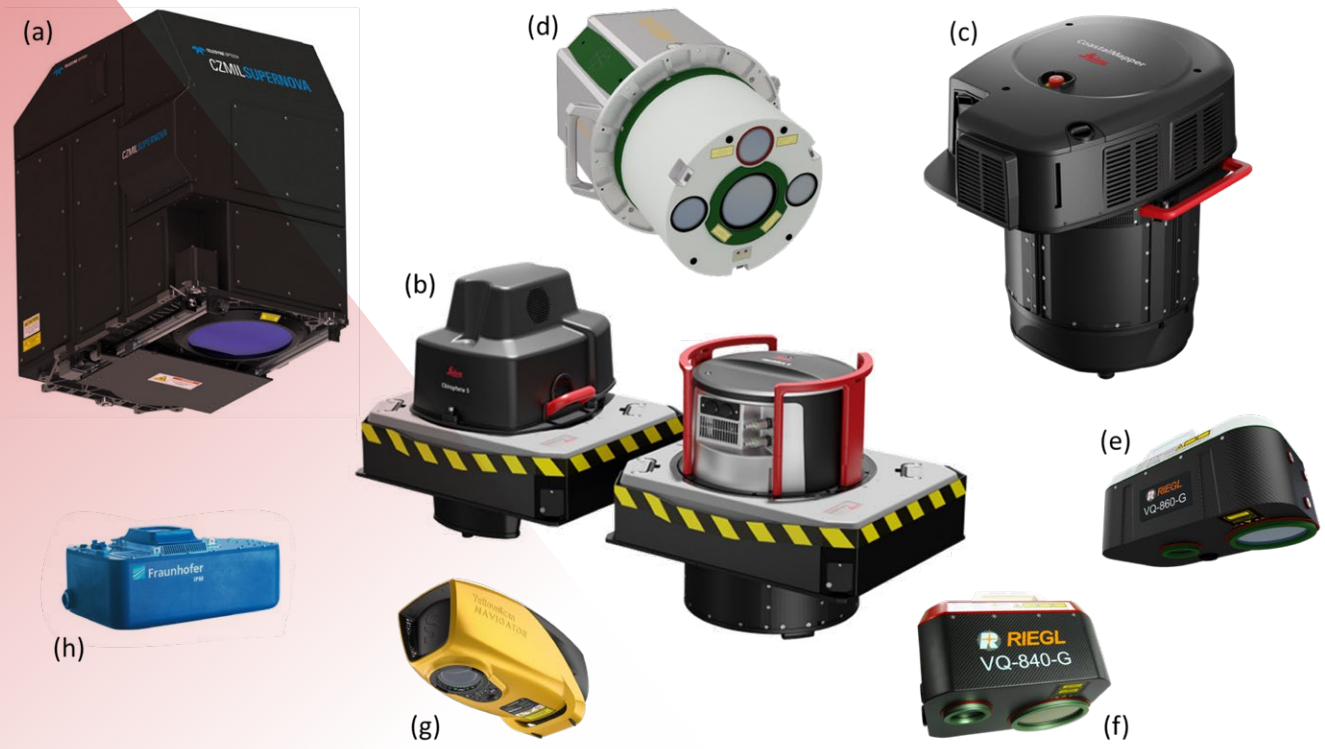

Figure 3: Gallery of commercially available topobathymetric laser scanners: (a) CZMIL SuperNova, (b) HawkEye-5, (c) CoastalMapper, (d) VQ-880-GII, (e) VQ-860-G, (f), VQ-840-GL, (g) Navigator, (h) ABS-SR.

which is limited due to the low flying altitudes and velocities of the drones and their limited flight endurance of approximately 20-30 minutes.

By far the largest group of sensors is operated from either fixed-wing aircraft or helicopters from typical flying altitudes of around 500-750 m. Most manufacturers of survey-grade topographic laser scanners also offer topobathymetric scanners (Teledyne Geospatial, Leica Geosystems, RIEGL Laser Measurement Systems). Scanners carried by aircraft weigh around 30-300 kg and are often equipped with cameras alongside the laser scanners. Some scanners either operate distinct deep channels for maximizing the depth penetration (3 SD) and one or more shallow channels for increasing the spatial resolution (1.5-2.5 SD). Most of the available scanners also provide an infrared (IR) laser channel, either as a separate scanner or in the classical concept with synchronous and coaxial emission with the green laser channel. These systems represent a compromise between good spatial resolution and high area coverage.

Table 1 summarizes the system parameters of selected state-of-the-art instruments operated from spaceborne, airborne, and UAV-borne platforms. If more than one green channel (λ=515/532 nm) is reported in **Table 1**, the first refers to the deep and the second to the shallow channel. The measurement rates and laser beam divergences follow the same ordering (green/deep, green/shallow, IR). The resulting laser footprint diameters are reported for the green channels only and mark the range of smallest and largest laser spot sizes considering the sensor's variation of beam divergence and flying altitude. **Figure 3** shows views of the instruments listed in **Table 1**.

CZMIL SuperNova (Teledyne Geospatial) and HawkEye-5 (Leica Geosystems) are examples of sensors equipped with distinct deep and shallow water channels plus an IR channel. CZMIL SuperNova uses a segmented FoV concept, where seven shallow water segments add up to the larger FoV of the deep channel. The instrument enables synchronous and coaxial emission of green and IR laser pulses. The deep channel of the CZMIL sensor has the highest reported penetration depth of 3 SD. The HawkEye-5 sensor

consists of two separate laser scanners: the HawkEye-5 deep module and the Chiroptera-5 for shallow water. The deep module features a good penetration depth of 2.5 SD at a moderate pulse repetition rate (PRR) of 40 kHz, and the shallow Chiroptera-5 penetrates 2 SD at a PRR of 200 kHz. Leica Geosystems has announced the CoastalMapper, a topobathymetric system consisting of a topographic scanner (Hyperion3) and a newly designed bathymetric scanner (Theia) integrated into a compound sensor head. The scanner maximizes the areal coverage rate for bathymetric surveys by providing a large FoV (50°) and a high flying altitude (800 m).

The VQ-800-G family from RIEGL LMS, in turn, feature the highest resolution of all aircraft- or helicopter based scanners. The VQ-880-GII provides a small laser footprint diameter of 42 cm at the lower flying altitude of 600 m and a high point density due the high pulse repetition rate of 700 kHz for the bathymetric scanner. The VQ-860-G is optimized for helicopter integration with a mass of less than 20 kg and features a user-selectable beam divergence of 1-6 mrad and receiver's FoV (3-18 mrad). This results in a laser spot size of 15 cm when flown at 150 m with the narrowest beam divergence of 1 mrad. The best depth penetration of 2.5 SD, however, is achieved with a low PRR (50 kHz) and wide laser beam (6 mrad). All scanners of the VQ-800-G family have a short pulse duration of around 1.5 ns, which is beneficial for measuring very shallow water depths of around 20 cm.

The intended carrier platform for the VQ-840-GL is a multicopter UAV. The instrument weighs less than 10 kg including GNSS and IMU and can be carried by drones with a maximum take-off-mass (MTOM) of 25-30 kg. With this sensor, very small laser footprints of less than 1 dm and high point densities of >50 points/m^2 can be realized when flying slow (e.g., 5 m/s), low (e.g., 50 m) and with a narrow beam (1 mrad). While the VQ-840-G has been available since 2018, more UAV-borne bathymetric laser scanners have emerged more recently. For example, the YellowScan Navigator is a very compact sensor weighing less than 4 kg with a penetration depth of 2 SD at a measurement rate of 20 kHz. This green-only system can be operated at altitudes between 50

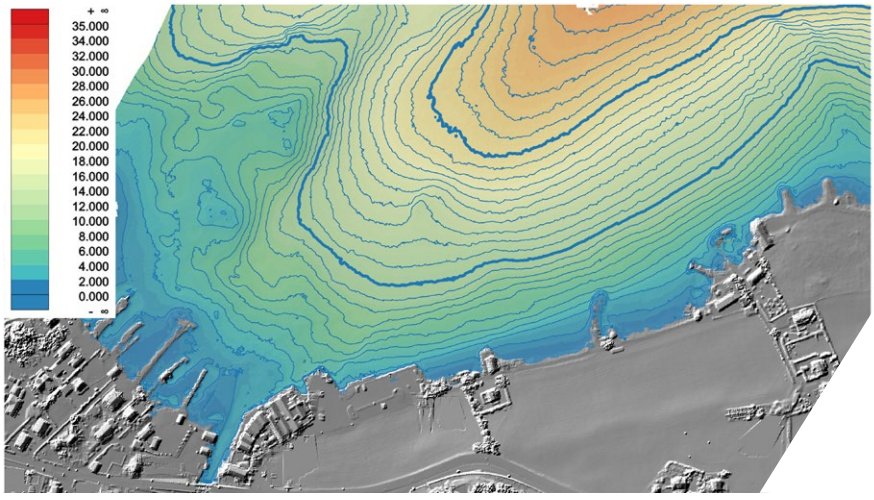

Figure 4: DEM hill shading superimposed with color-coded water depth map and depth isolines (isoline intervals 1 and 10 m), derived from Teledyne Optech CZMIL Supernova data

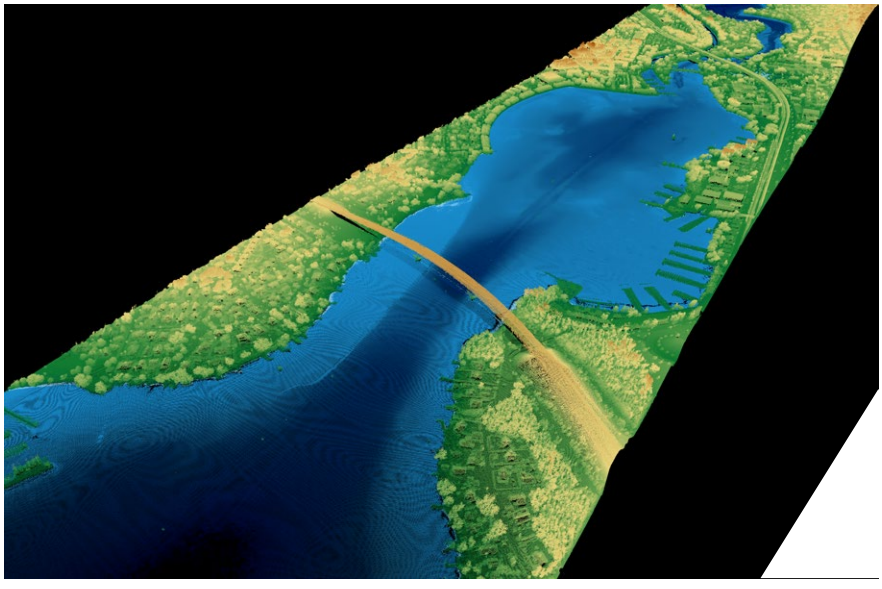

Figure 5:: Color-coded 3D point cloud of a flight strip captured with the Leica CoastalMapper sensor.

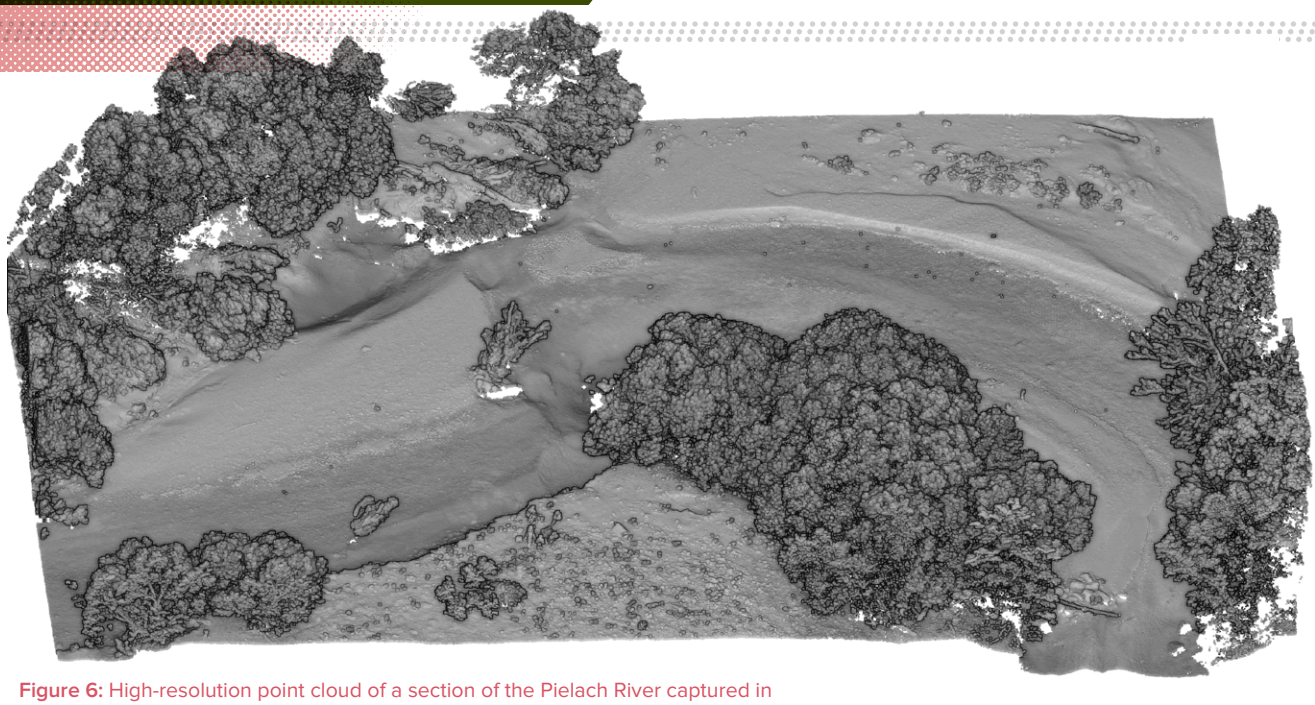

Figure 6: High-resolution point cloud of a section of the Pielach River captured in October 2024 with a RIEGL VQ-840-GL topobathymetric UAV laser scanner.

and 100 m. The short-range Airborne Bathymetric Scanner (ABS-SR) from Fraunhofer IPM is designed for low flight altitudes of 15 m. The scanner synchronously emits green and IR pulses as used in the classic ALB concept. Since the beam widening takes place via lenses in the instrument, the scanner delivers a laser beam with a constant diameter of 5 cm. This makes the sensor particularly interesting for detecting small objects such as underwater vegetation, piles or small boulders.

Examples of topobathymetric data sets

Figure 4 shows a DEM hill shading superimposed with a color-coded water depth map and 1 m depth isolines derived from topobathymetric CZMIL SuperNova data (Teledyne Geospatial)[1]. With the deep channel, it was possible to penetrate to a depth of more than 30 m. The topographic channel and the multiple shallow water channels deliver high-resolution topography in the dry-land part of the scene.

Figure 5 shows a color-coded 3D point cloud of a single flight strip captured with the Leica CoastalMapper sensor. The data was collected during a test flight with a swath width of 800 m and processed with Leica HxMap software. The point cloud shows a seamless transition from water to land and full coverage of topography, vegetation, buildings, and bathymetry[2].

The final example, shown in **Figure 6**, depicts a high-resolution 3D point cloud of a section of the pre-alpine Pielach River in Austria captured in October 2024 with the RIEGL VQ-840-GL topobathymetric UAV laser scanner[3]. Brighter tones in the plot depict higher reflectance. The plot shows all points classified as dry ground, vegetation, and water bottom. For better readability, points classified as water surface, water column, and outliers were discarded. **Figure 6** demonstrates the benefits of the very high spatial resolution (high point density, small laser footprint). For example, occasional small boulders in the riverbed as well as submerged vegetation in the middle of the river can clearly be identified in the point cloud. This opens a path to detailed hydrodynamic-numerical modeling and habitat mapping.

Selected applications

The range of ALB applications is broad and continually expanding, driven by advances in sensor versatility and miniaturization. Key applications include:

- Underwater object detection: ALB was originally developed for military use in detecting submerged objects. Today, it is widely applied in civil maritime operations, including

1 The data was collected during a calibration flight near the island of Fjøløy (Stavanger, Norway) and kindly provided by the company Field.

2 The image was kindly provided by Leica Geosystems.

3 The data of this example is available as open research data (DOI: 10.48436/taz19-r6618).

harbor security, safe navigation of autonomous underwater vehicles, and monitoring of coastal safety. The detection of small objects requires advanced waveform analysis techniques. The use of UAV-borne ALB has further improved resolution, allowing for the identification of features such as boulders or man-made debris.

- 3D Mapping of submerged topography: Mapping underwater terrain remains the primary use of ALB. It is crucial for creating accurate nautical charts, particularly in shallow coastal and harbor areas. Advances in technology have improved depth penetration, and even satellite-based systems now contribute to near-shore bathymetry. For smaller inland water bodies such as rivers and lakes, high-resolution topobathymetric sensors mounted on crewed or remotely piloted platforms provide the necessary detail. In addition, ALB data is increasingly being integrated systematically into national and regional mapping efforts.
- Ecological applications: ALB supports environmental monitoring in both coastal zones and inland water bodies. It is used to estimate seafloor reflectance and to detect, classify, and model benthic habitats. These capabilities are valuable for habitat conservation and management, as well as for river restoration projects. The ecological relevance of ALB continues to grow, especially in the context of international environmental directives and frameworks.
- Coastal and fluvial geomorphology: ALB is used to analyze both long-term changes and short-term dynamics, such as those induced by hydropeaking. Its high spatial resolution makes it a valuable tool for studying erosion, sediment transport, and river morphology. ALB data also forms the basis for hydrodynamic and flow simulations, supporting a variety of water-related engineering and environmental applications.
- Turbidity estimation: Though turbidity limits the depth to which ALB can penetrate, it also represents a valuable environmental parameter. ALB systems, especially those capable of full-waveform analysis, can be used to estimate water turbidity and assess water quality, supporting ongoing monitoring efforts.
- Risk assessment and disaster management: As extreme weather events become more frequent due to climate change, timely and detailed mapping of coastal and floodplain areas is critical. ALB contributes to both pre- and post-event assessments, offering valuable data for disaster preparedness, response, and recovery. It complements other remote sensing and in-situ measurement methods in comprehensive risk management strategies.
- Macrophyte detection and mapping: We are facing rapid changes in the structure and composition of underwater vegetation, accelerated by climate change. Detection, mapping and monitoring requires the use of high-resolution sensors and agile platforms operating from low altitudes. UAV-based laser scanners are the ideal solution. Their concepts and applications are the focus of the fourth and final part of the airborne lidar tutorial.

Dr. Gottfried Mandlburger studied geodesy at TU Wien, where he also received his PhD in 2006 and habilitated in photogrammetry with a thesis on "Bathymetry from active and passive photogrammetry" in 2021. In April 2024 he was appointed University Professor for Optical Bathymetry at TU Wien.

His main research areas are airborne topographic and bathymetric lidar from crewed and uncrewed platforms, multimedia photogrammetry, bathymetry from multispectral images, and scientific software development. Gottfried Mandlburger is chair of the lidar working group of Deutsche Gesellschaft für Photogrammetrie, Fernerkundung und Geoinformation e.V. (DGPF) and Austria's scientific delegate in EuroSDR. He received best paper awards from ISPRS and ASPRS for publications on bathymetry from active and passive photogrammetry.

Further reading

Abdallah, H., N. Baghdadi et al., 2012. WaLiD. A new lidar simulator for waters, *IEEE Geoscience Remote Sensing Letters,* DOI: 10.1109/LGRS.2011.2180506.

Guenther, G., A. Cunningham, P. Laroque and D. Reid, 2000. Meeting the accuracy challenge in airborne lidar bathymetry, *Proceedings of the 20th EARSeL Symposium: Workshop on Lidar Remote Sensing of Land and Sea,* Dresden, Germany.

Mandlburger, G., 2020. A review of airborne laser bathymetry for mapping of inland and coastal waters, *Journal of Applied Hydrography*, 116: 6–15.

Parrish, C.E., L.A. Magruder et al., 2019. Validation of ICESat-2 ATLAS bathymetry and analysis of ATLAS's bathymetric mapping performance, *Remote Sensing*, DOI: 10.3390/rs11141634.

Philpot, W. (ed.), 2019. *Airborne Laser Hydrography II*, Cornell University Library (eCommons), Cornell. https://ecommons.cornell.edu/handle/1813/66666.